Electronic Supplementary Material (ESI) for Sustainable Energy & Fuels.

Supporting Information†

Mesoporous Carbon-Supported Manganese Tungstate Nanostructure for the Development of Zinc-Air Battery Powered Long Lifespan Asymmetric Supercapacitor

Sourav Mallick, Arpan Samanta and C. Retna Raj*
Functional Materials and Electrochemistry Lab, Department of Chemistry, Indian Institute of

Technology, Kharagpur, India

E-mail: **crraj@chem.iitkgp.ac.in**

The mass to charge balance of the two electrodes of asymmetric supercapacitor device:

$$C_{m+} \Delta V_{+} m_{+} = C_{m-} \Delta V_{-} m_{-} \quad (1)$$

Where, C_{m+} and C_{m-} are the specific capacitances (F g^{-1}), ΔV_{+} and ΔV_{-} are the potential windows (V) and m_{+} and m_{-} are the mass loading of the positive and negative electrodes, respectively.[1]

Calculation of specific capacitance (C_{sp}), energy density (E), power density (P) and coulombic efficiency of the asymmetric device:

$$C_{sp} = \frac{I\Delta t}{A\Delta V}\ mFcm^{-2} \quad (2)$$

$$E = \frac{C\Delta V^2}{2}\ mWhcm^{-2} \quad (3)$$

$$P = \frac{E}{\Delta t}\ mWcm^{-2} \quad (4)$$

where C (F cm^{-2}) is the specific capacitance, I (mA) represent the discharge current, A (cm^{-2}) designates total area of the electrodes, ΔV (V) and Δt (s) are the cell voltage and total discharge time, respectively.[1]

Coulombic efficiency (η) was calculated using the formula [1]:

$$\eta = \frac{\Delta t_d}{\Delta t_c} \times 100 \quad (5)$$

where, Δt_c and Δt_d are the time taken for completely charge and discharge of the device, respectively. [1]

Koutecky–Levich (K-L) equation and Tafel analysis:

The polarization curves were obtained at different rotation and further analyzed according to Koutecky–Levich (K-L) equation[2]

$$\frac{1}{J} = \frac{1}{J_D} + \frac{1}{J_K} \quad (6)$$

$$\frac{1}{J} = \frac{1}{0.69\, n\, F\, C_0 D^{\frac{2}{3}} v^{-\frac{1}{6}} \omega^{\frac{1}{2}}} + \frac{1}{nFkC_0} \quad (7)$$

where, J_K is kinetic and J_D is the diffusion limited current density. 'ω' is the angular velocity, 'F' is Faraday's constant, 'C_0' (0.00118 mM cm^{-3}) is the concentration of dissolved oxygen, 'D' (1.00009 $cm^2\ s^{-1}$) is the diffusion coefficient of oxygen, 'n' is the number of electrons transferred, 'v' (0.01 $cm^2 s^{-1}$) is the kinematic viscosity of solution and 'k' is the apparent electron transfer rate constant.

The kinetics of ORR was further studied by Tafel analysis, by using the following equation[2]

$$J_k = (J_{lim} \times J_{diff})/(J_{lim} - J_{diff}) \quad (8)$$

Calculation of n value and % HO_2^-:

The n value and % HO_2^- were obtained from the RRDE profile at 1600 rpm according to the standard procedures.[2]

$$n = 4NI_D /(NI_D+I_R) \quad (9)$$

$$\% HO_2^- = 200I_R/(NI_D+I_R) \quad (10)$$

where, I_D and I_R are the disk and ring current respectively and N is the current collection efficiency of RRDE (0.37).

Fig. S1. (a) BET profile and (b) BJH pore-size distribution plot of cotton fabric (200 GSM) derived mesoporous carbon.

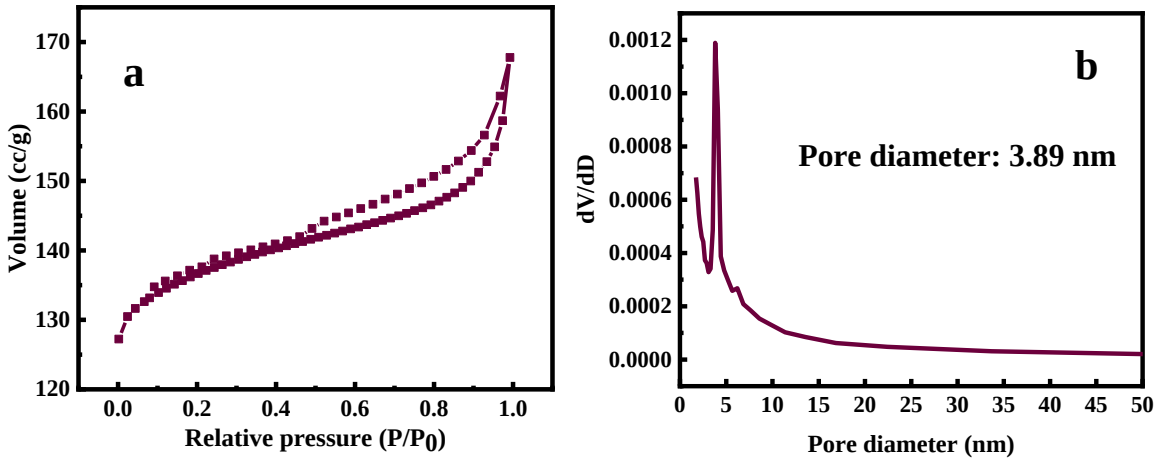

Fig. S2. XPS surface survey scan profile of $MnWO_4$/CC.

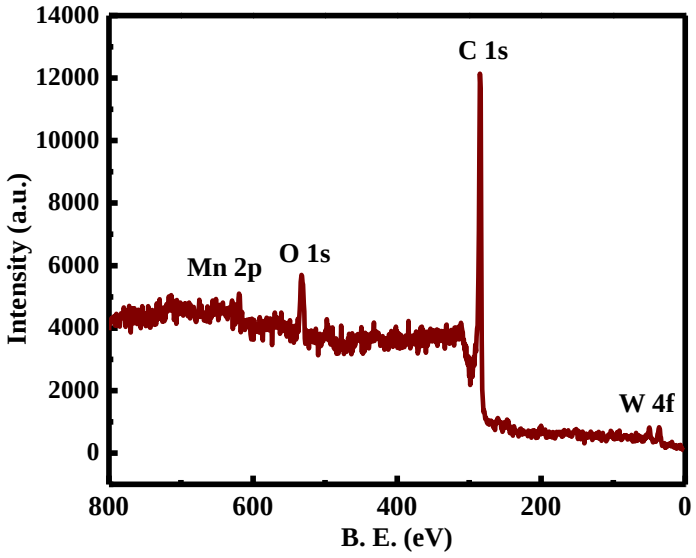

Fig. S3. FESEM images of $MnWO_4$/CC at low magnification.

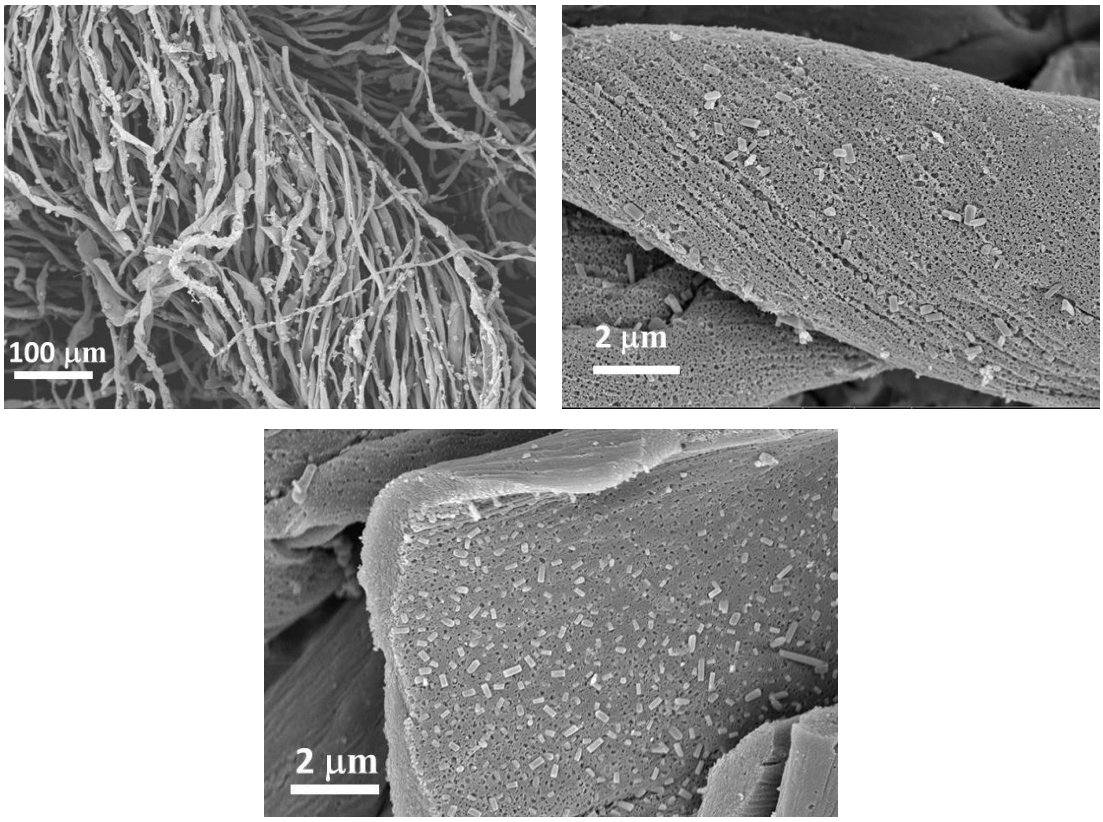

Fig. S4. EDS analysis and atomic percentages of each elements of $MnWO_4$/CC.

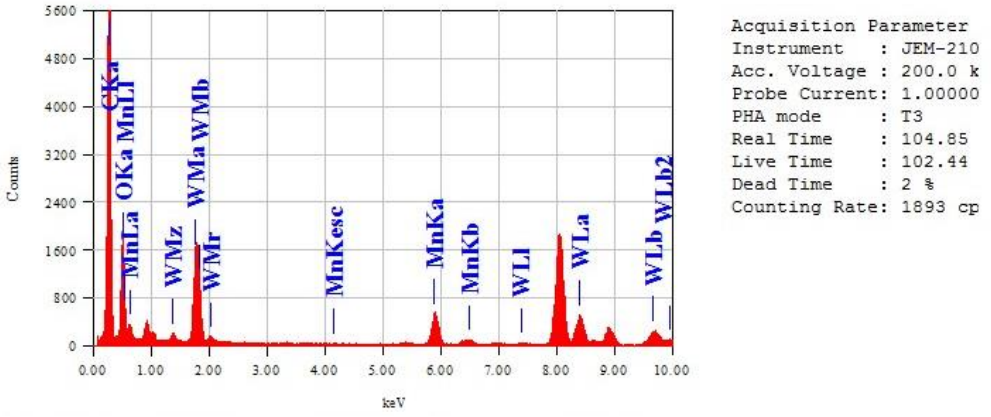

Elements name	Atomic (%)
C	86.90
O	9.78
Mn	1.58
W	1.74
Total	100.00

Fig. S5. XRD profile and FESEM images of carbon-free $MnWO_4$ obtianed at different temperature.

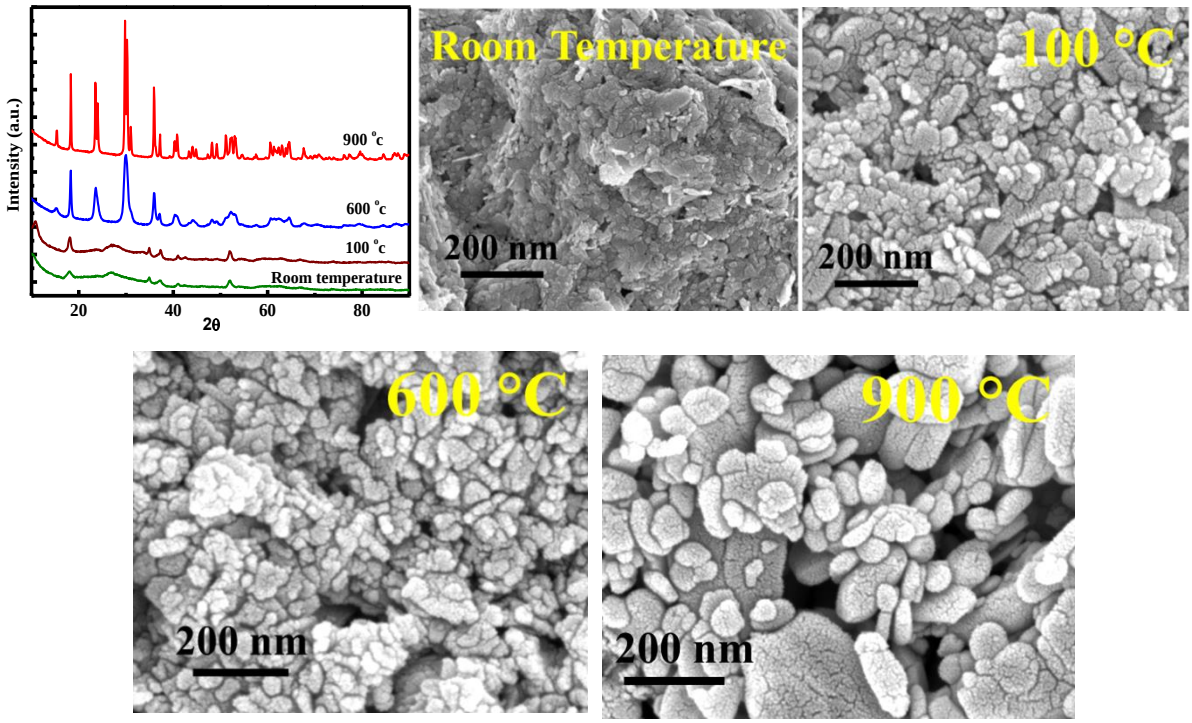

Fig. S6. (a) Cyclic voltammetric profile of $MnWO_4$/C coated Ni foam at different scan rates. (b) Comparative cyclic voltammetric and (c) charge- discharge profiles of $MnWO_4$/C, $MnWO_4$ and C (200 GSM) coated Ni foam.

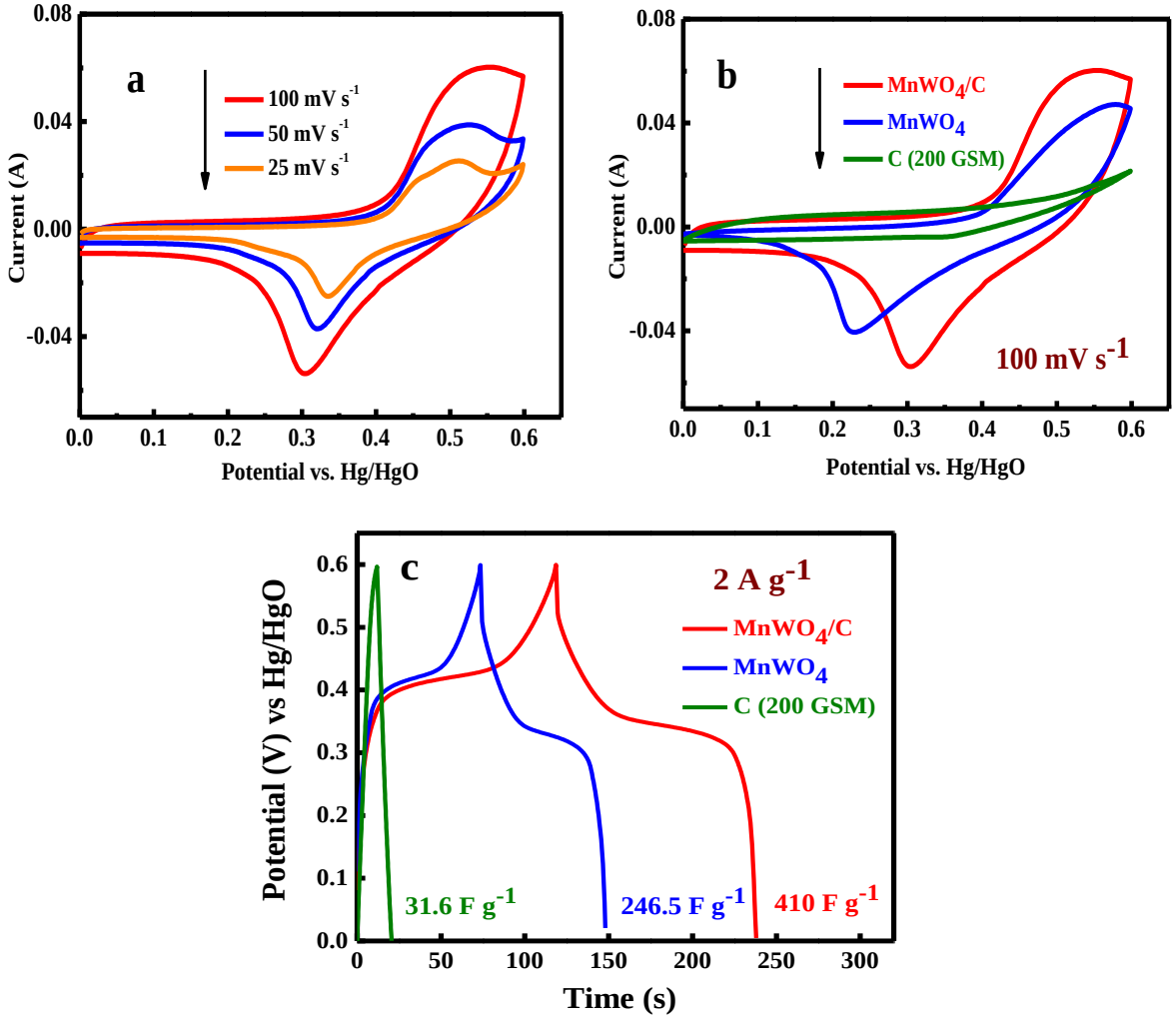

Fig. S7. (a**)** Cyclic voltammetric and (b) charge-discharge profiles of negative electrode material (carbon derived from 600 GSM cotton fabric) obtained with three-electrode system.

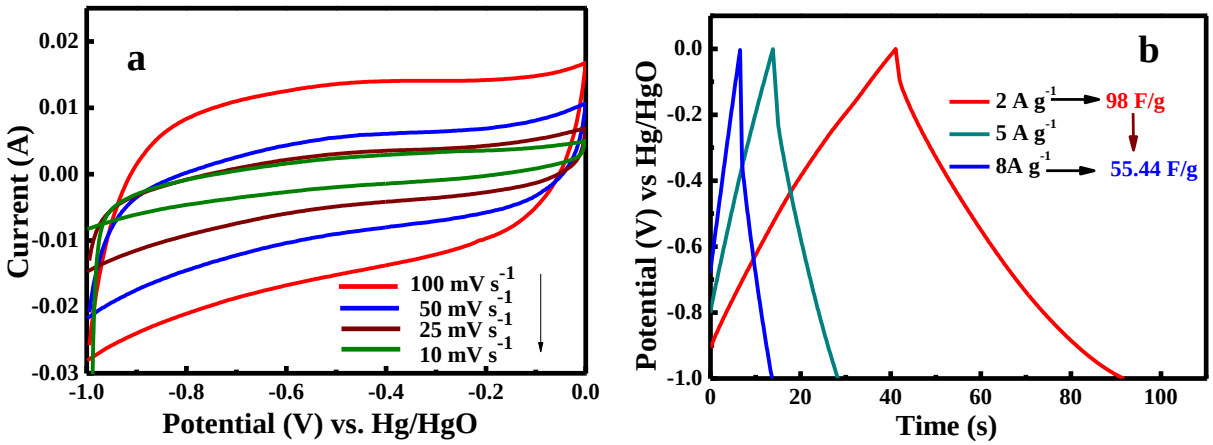

The mass to charge balance calcultion based on the performnce of $MnWO_4$/C and bare C (600 GSM):

$m_-/m_+ = (C_{m+}\Delta V_+)/(C_{m-}\Delta V_-) = (410 \times 0.6)/(98 \times 1) = 2.51$

The bare 600 GSM cotton fabric derived CC was choosen for negative electrode, having thread count ~3 times higher than 200 GSM cotton fabric (GSM= grams per square meter)

Fig. S8 Plot illustrating the (a) rate capability, (b) energy and power density (Ragone plot) of the asymmetric device.

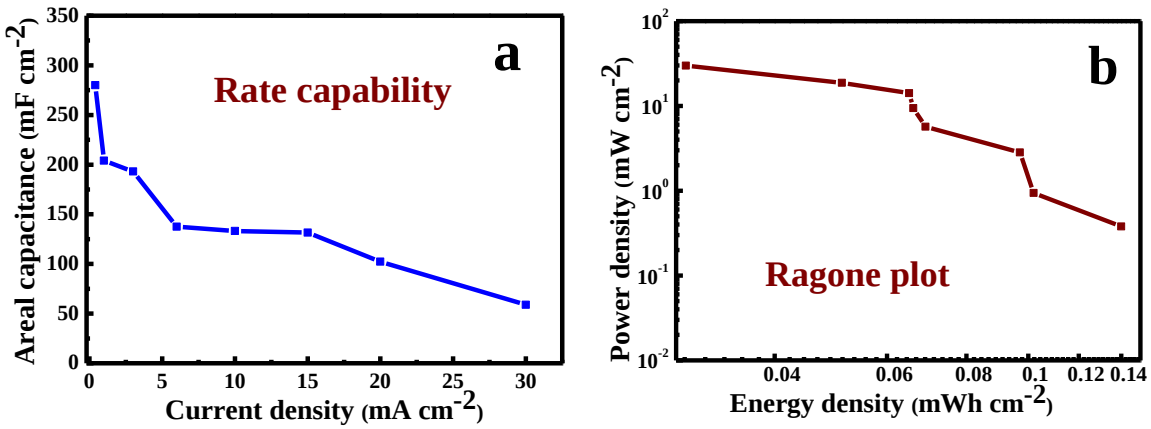

Fig. S9 Digital photograph of glowing 29 Red LEDs of varying intensity at different time interval.

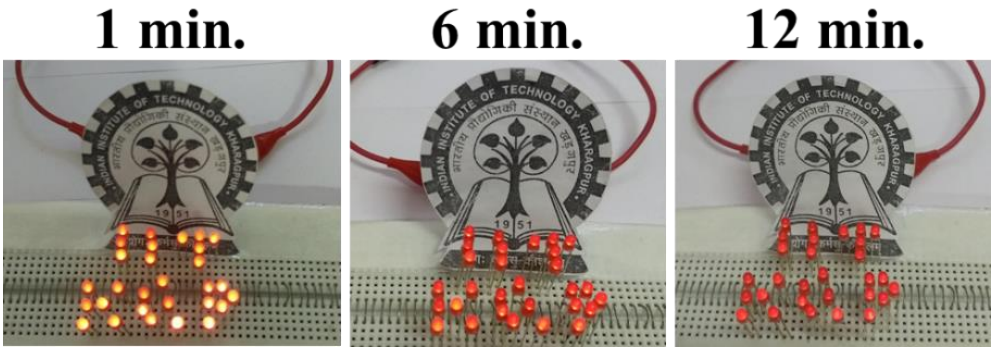

Fig. S10. Charge-discharge cycling performance of asymmetric device at the current density of 20 mA cm^{-2} for 50,000 cycles. Selected region is given for clarity reason.

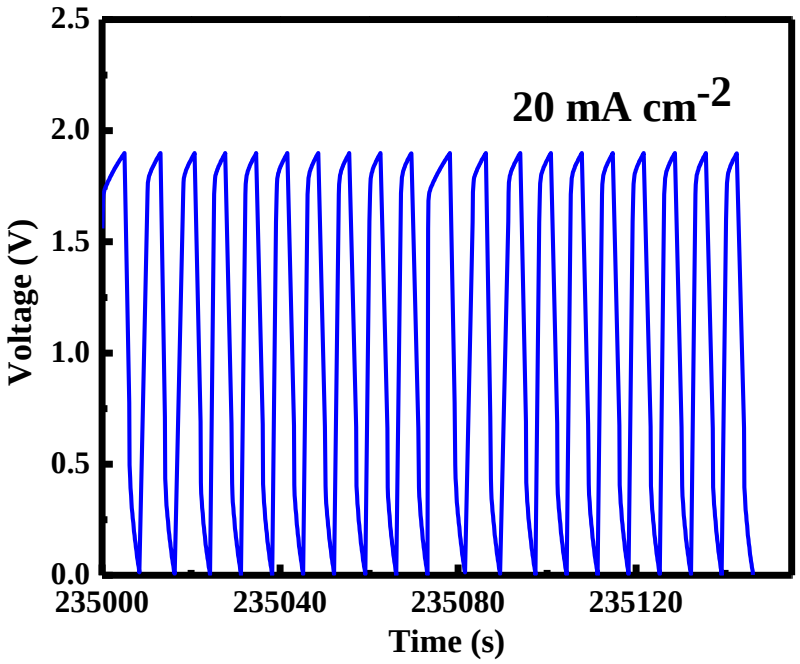

Fig. S11. (a) Plot of phase angle vs log (frequency) and (b) C″ vs. log (frequency) of the device before and after cycling.

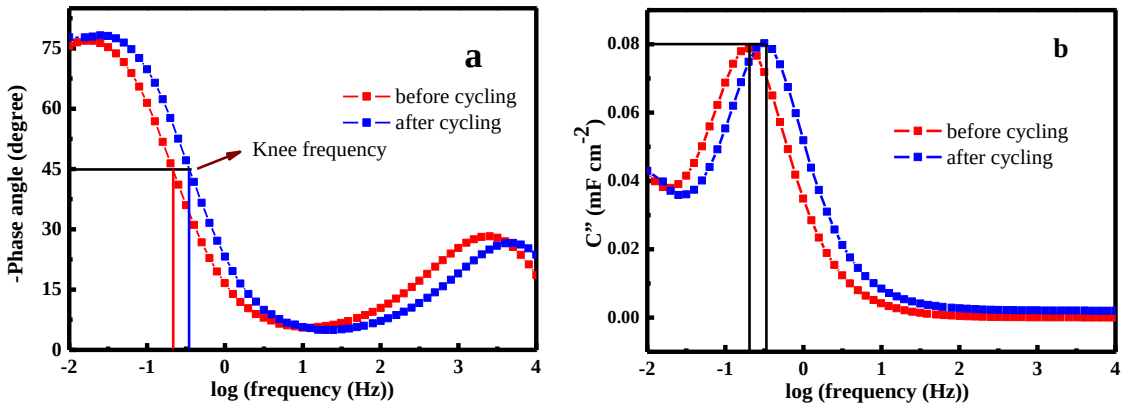

Fig. S12. Post-cycling TEM image of $MnWO_4$/CC. Measurement was performed with the electrode material after 50,000 cycles.

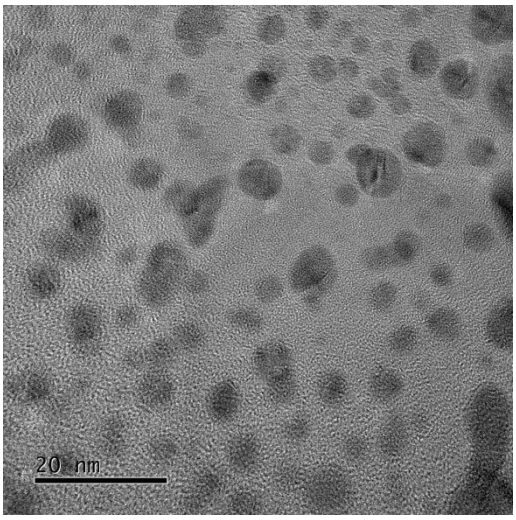

Fig. S13. Post-cycling STEM mapping images of $MnWO_4$/CC.

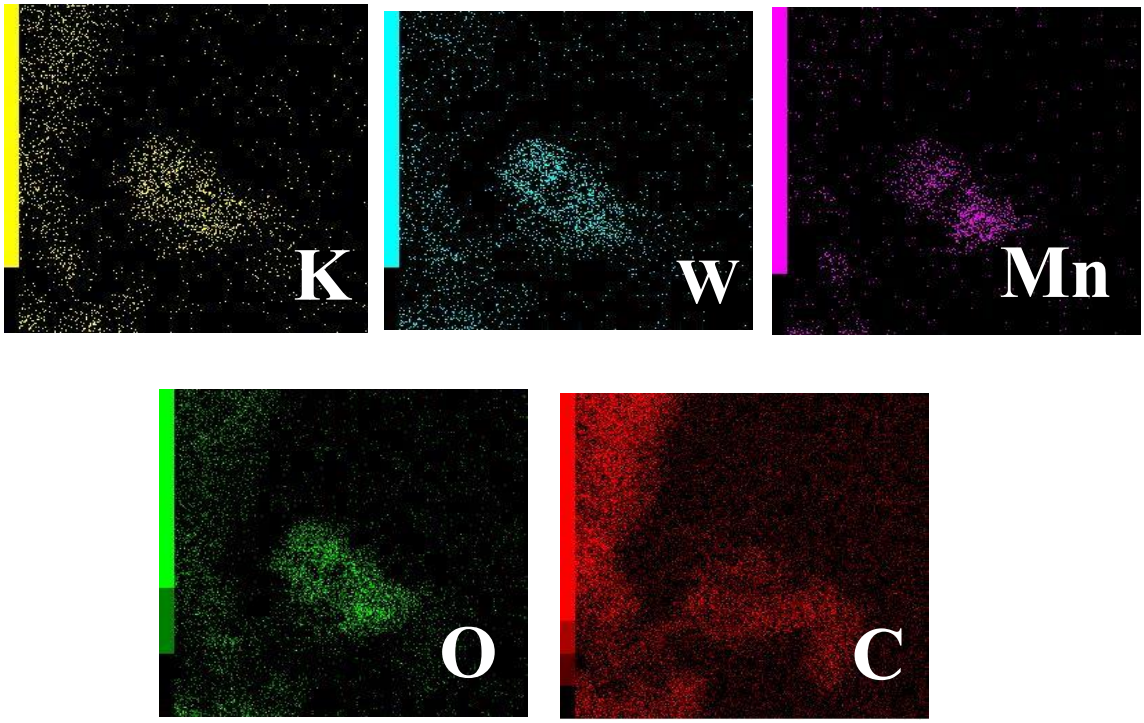

Fig. S14. EDS analysis and atomic percentages of each elements of $MnWO_4$/CC after durability test.

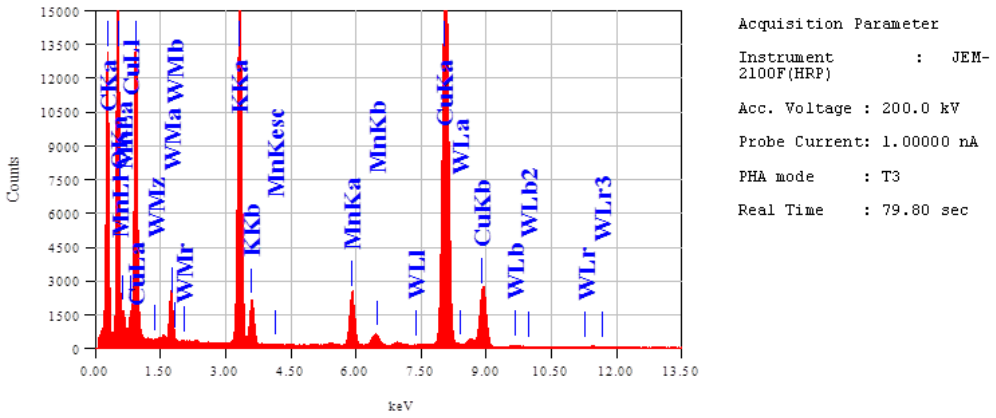

Elements name	Atomic (%)
C	50.98
O	31.35
Mn	2.85
W	5.01
K	9.81
Total	100.00

Fig. S15. Electrochemical surface area (ECSA) of $MnWO_4$/C, $MnWO_4$ and mesoporous carbon.

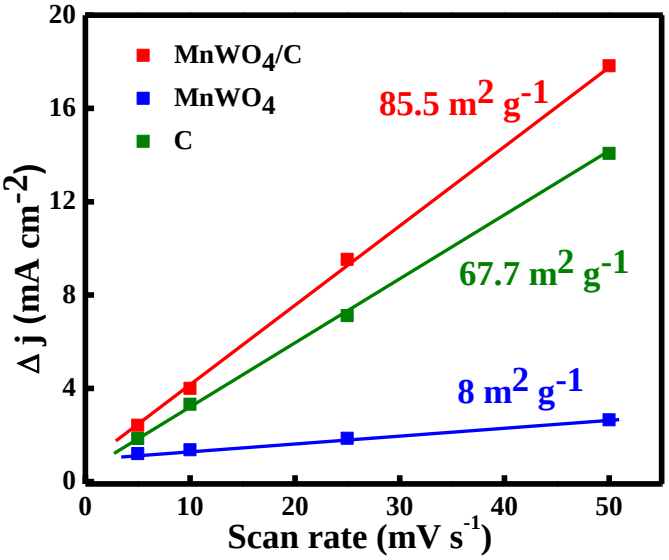

Calculation of ECSA:[3,4]

ECSA= C_s/(40 μF cm^{-2} per cm^2_{ECSA})

Mass specific ECSA = (ECSA/ catalyst loading)

Where, C_s = double layer capacitance (slop of the Δ j vs. scan rate plot)

The specific capacitance for a flat surface is generally found to be in the range of 20-60 μF cm^{-2}.

Fig. S16. (a) Polarization curves for ORR, (b) plot illustrating the ORR activity in terms of current density and (c) tafel plot for the as-synthesized carbon-free $MnWO_4$, mesoporous carbon (C), $MnWO_4$/C and 20% Pt/C. (d) Plot illustrating the durability as-synthesized carbon-free $MnWO_4$ and $MnWO_4$/C.

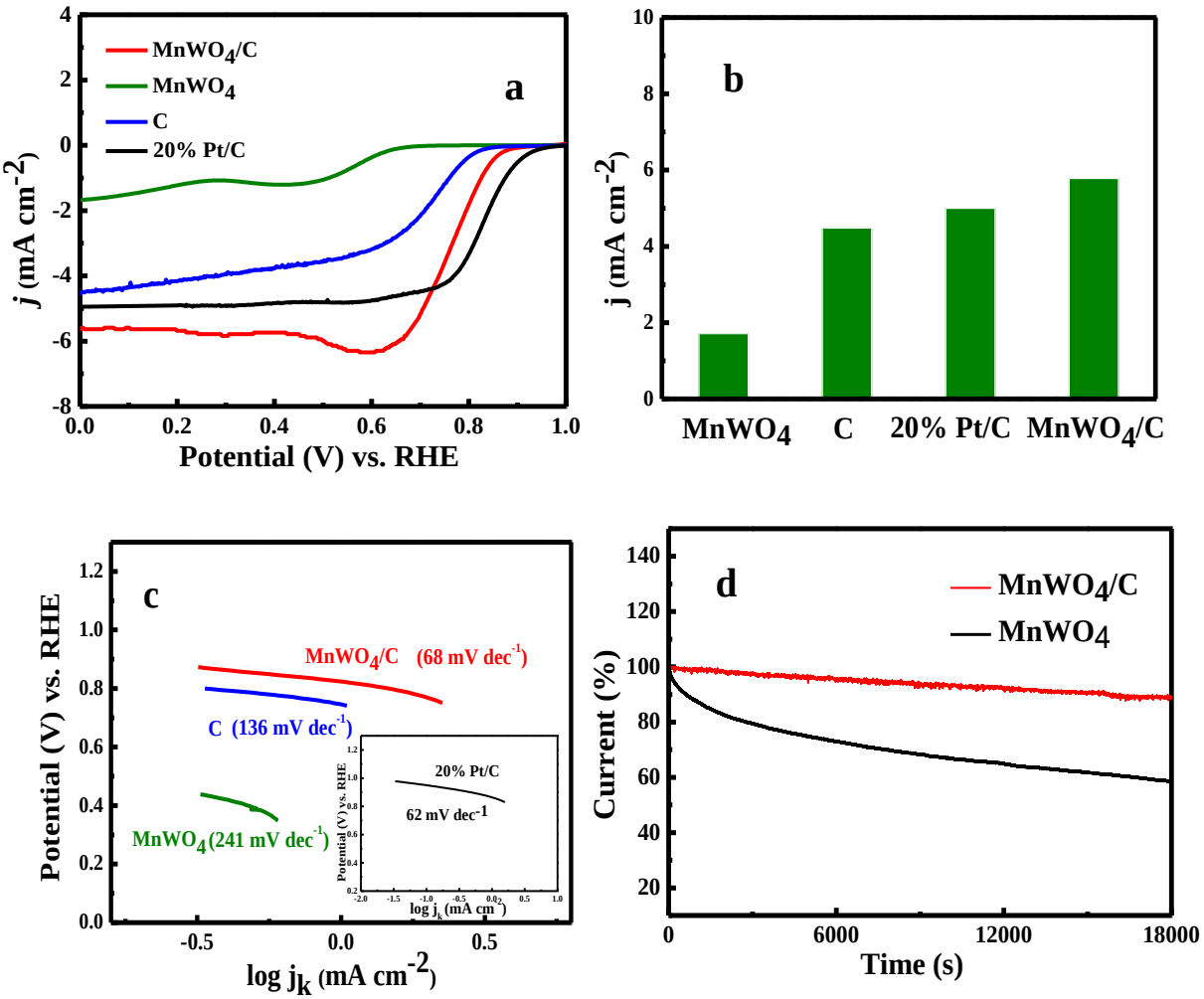

Fig. S17. (a) The polarization curve at varying rotation speed and (b) K-L plot at different potentials for $MnWO_4$/C.

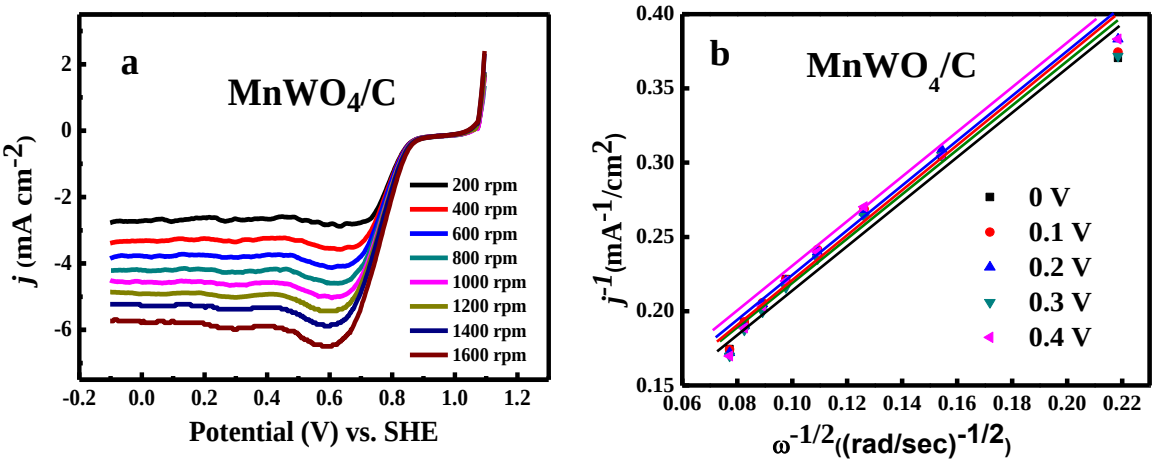

Fig. S18. The polarization curve at different rotation and K-L plot at different potentials for $MnWO_4$ (a,b), mesoporous carbon (c,d) and 20% Pt/C (e,f).

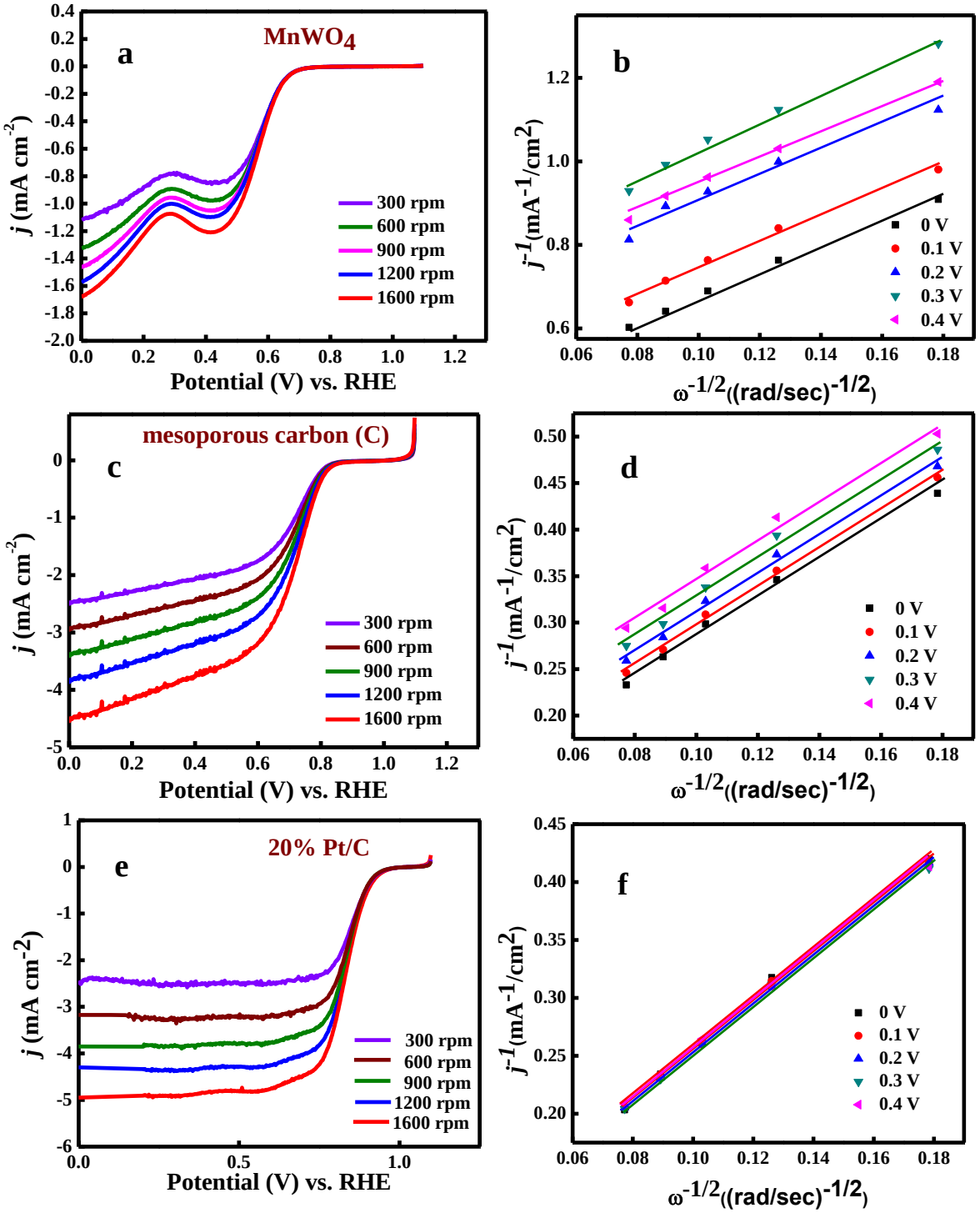

Fig. S19. (a) The RRDE profile of $MnWO_4$/C. (b) Comparative n value and % HO_2^- of $MnWO_4$/C, $MnWO_4$ and mesoporous carbon (C).

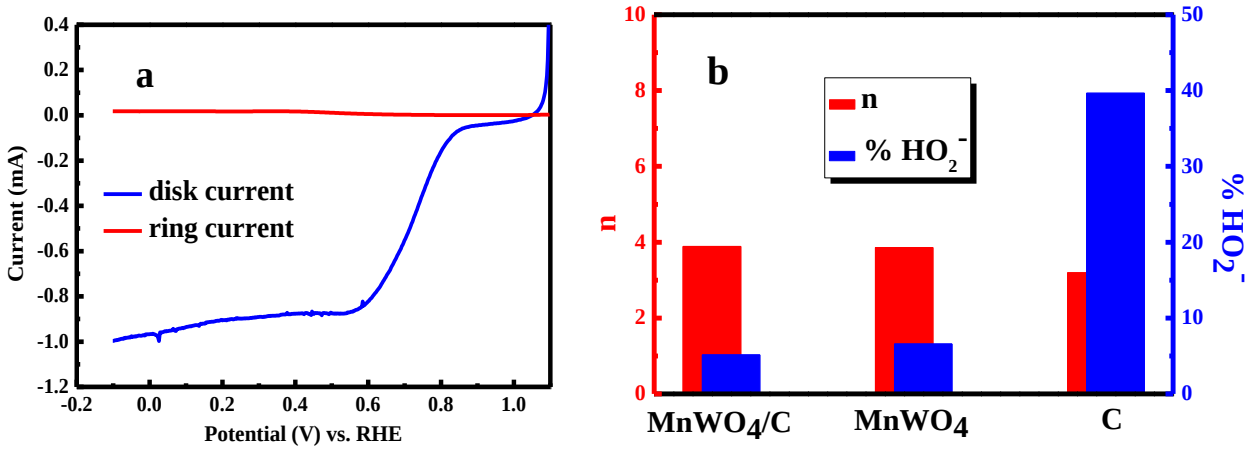

Fig. S20. Charge-dishcarge cycling performance of reference catalyst 20% Pt/C+ IrO_2 based Zn-air battery.

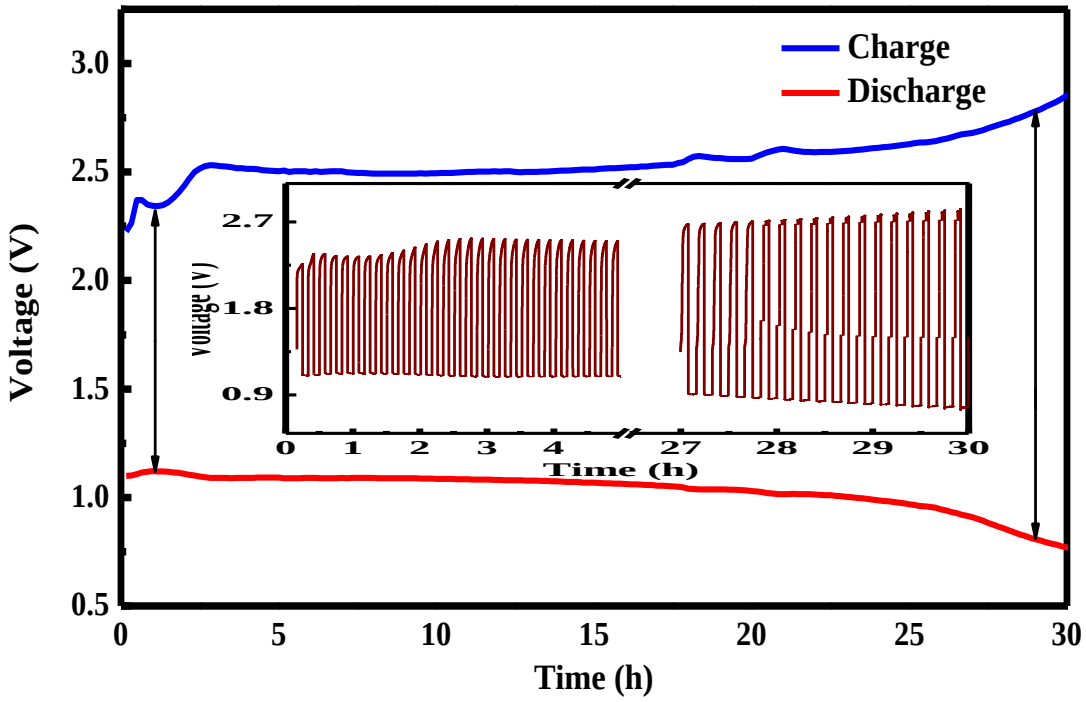

Fig. S21. Discharge profile of ZAB at 50 mA cm^{-2}.

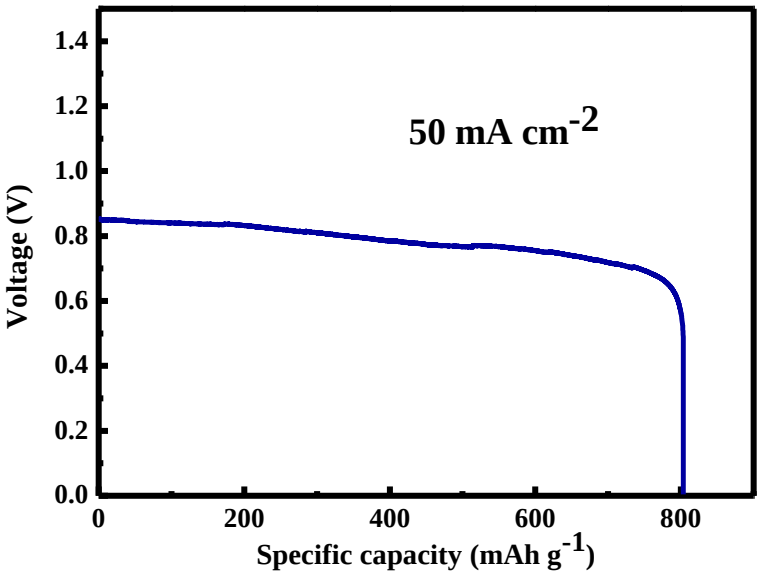

Fig. S22. Plot illustrating the charge-discharge cycling stability of meshed coin cell based ZAB.

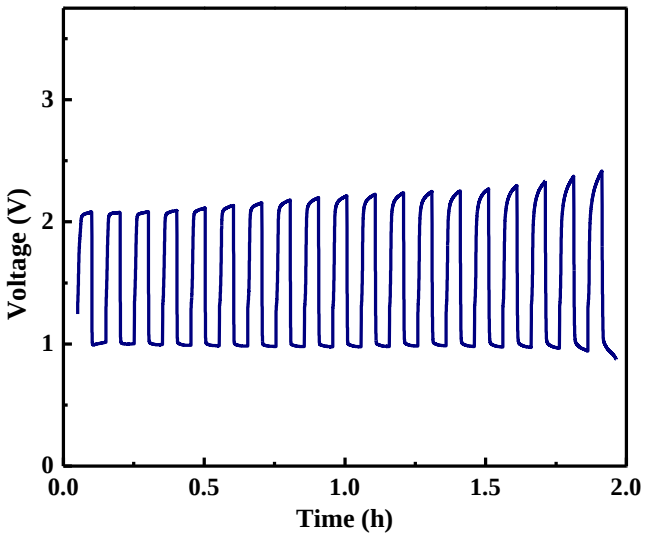

Table S1. Supercapacitive performance of $MnWO_4$ based material in the literature.

Materials	Electrolyte & potential window	Three electrode performance	Two electrode performance	Durability	References
$MnWO_4$	1 M KOH	219 F g^{-1} at 0.4 A g^{-1} (0 - 0.6 V vs. Hg/HgO)	-	increased after 3000 cycles	*Mater. Chem. Phys.* **2015**, 167, 22.
$MnWO_4$ Nanorods (hydrothermal synthesis)	3 M KOH	256 F g^{-1} at 0.4 A g^{-1} (0 - 0.5 V vs. Ag/AgCl)	-	62% after 1200 cycles	C*hemistrySelect* **2017**, 2, 5707.
$MnWO_4$ nanorods (using CTAB)	1 M H_2SO_4	16 F g^{-1} at 1.3 mA cm^{-2} (0 – 1.2 V vs. Ag/AgCl)	-	increased after 1000 cycles	*J Electroceram* **2012**, 28, 220.
$MnWO_4$ (using DNA scaffold)	0.1 M Na_2SO_4	34 F g^{-1} at 0.5 mA cm^{-2} (0 – 1 V vs. SCE)	-	Not mentioned	*RSC Adv*. **2014**, 4, 38169
$MnWO_4$/rGO (hydrothermal synthesis)	6 M KOH	261 F g^{-1} at 0.5 A g^{-1} (-0.35 – 0.55 V vs. Ag/AgCl)	(0 - 1.5 V) 101 F g^{-1} at 0.5 A g^{-1}	85.1% after 6000 cycles	*J. Alloys Compd* **2016**, 666, 15.
$MnWO_4$ microflower	0.1 M Na_2SO_4	324 F g^{-1} at 1 mA cm^{-2} (0 - 1 vs. Ag/AgCl)	(0 - 1.8 V) 34 Wh kg^{-1} at 500 W kg^{-1}	84% after 3000 cycles	*Int. J. Hydrogen Energ.* 2019, 44, 10838.
WO_3@$MnWO_4$ core-shell	0.5 M H_2SO_4	550.9 F g^{-1} at 2 A g^{-1} (-0.65 – 0 V vs. Ag/AgCl)	0 - 2 V 152.4 Wh kg^{-1} 3583.5 kW kg^{-1}	92% after 10,000 cycles	*J. of Colloid Interface Sci.* **2018**, 531, 216.
$MnWO_4$/CC	**3 M KOH 0 – 1.9 V**	**410 F g^{-1} at 2 A g^{-1} (0 – 0.6 V vs.Hg/HgO)**	**0.140 mWh cm^{-2} at 0.37 mW cm^{-2} 281.33 mF cm^{-2} (93.77 F g^{-1}) at 0.4 mA cm^{-2}**	**2% increase after 50,000 cycles**	**Our work**

Table S2. ECSA of the catalysts.

Catalyst	**ECSA (cm^2)**	**Mass specific ECSA ($m^2\ g^{-1}$)**
$MnWO_4$/C	8.55	85.5
$MnWO_4$	0.8	8.0
C-200	6.76	67.7

Table S3. Onset and half-wave potential of the catalysts.

Catalysts	**Onset (V vs. RHE)**	**$E_{1/2}$ (V vs. RHE)**
$MnWO_4$/C	0.89	0.76
$MnWO_4$	0.68	0.55
C-200	0.84	0.72
20% Pt/C	0.94	0.83

Table S4. ZAB performance of oxide-based material in the literature.

Catalyst	OCV (V)	Power density (mW/cm^2)	Stability	References
Mn_3O_4/N-CNT	Not given	133	50 h	*Batteries & Supercaps* 2019, *2*, 882 –893
CoO/NG	Not given	135	40 h	*ACS Sustainable Chem*. DOI: 10.1021/acssuschemeng.9b05492
Co-NiO NFs	Not given	93	20 h	*Appl. Catal. B Environ*. **2019**, *250*, 71–77
$MnCo_2O_4$@C	1.43 V	~40	70 h	*J. Power Sources* **2019**,*430*, 25-31
Mn-Co mixed oxide	1.53	108	30h	*Electrochim. Acta* **2016**, *211*, 735.
NiFeO@MnO*x* core–shell structures	Not given	81	100 cycle	*ACS Appl. Mater. Interfaces* ***2017***, *9, 8121*.
MnO_2/Co_3O_4	Not given	36	7 h	*Nanoscale* **2013**, *5*, 4657.
$MnWO_4$/C	**1.50 V**	**131**	**72 h (432 cycle)**	**Our work**

References

1. B. E. Conway, Electrochemical Supercapacitors: Scientific Fundamentals and Technological Applications, Kluwer Academic/Plenum Publisher, New York, 1999**.**

2. S. Mondal, C. R. Raj, *J. Phys. Chem. C* 2018, **122**, 18468.

3. J. Kibsgaard, C. Tsai, K. Chan, J. D. Benck, J. K. Nørskov, F. A. Pedersen, T. F Jaramillo, *Energy Environ. Sci.* 2015, **8**, 3022.

4. A. Tiwari, V. Singh and T. C. Nagaiah, *J. Mater. Chem. A*, 2018, **6**, 2681.